Ground-Based Augmentation System Antenna Array Size Reduction via Self-Cardioid Element

James A. Quinlan [1] and Daniel N. Aloi [2]

[1,2] Department of Electrical and Computer Engineering
Oakland University, Rochester, Michigan 48309, USA
jaquinla@oakland.edu, aloi@oakland.edu

Abstract ─ A Ground-Based Augmentation System (GBAS) monitors the signals of Global Navigation Satellite Systems and broadcasts differential correction signals. It relies on Multipath Limiting Antennas (MLAs) that can receive signals over almost the entire upper hemisphere while greatly attenuating signals reflected from the ground. The current Federal Aviation Administration (FAA)-approved system utilizes an MLA that is approximately 182.9 cm tall. In this paper, a substitute MLA is designed that is only 97.05 cm tall (approximately 44% reduction). The size reduction is accomplished by reducing the number of array elements from 19 to 11. We developed a novel self-cardioid antenna element that allows for this reduction.

Index Terms ─ Antenna array synthesis, antenna design, array size reduction, cardioid pattern, global positioning system, ground-based augmentation system, multipath limiting antenna.

I. INTRODUCTION

A Ground-Based Augmentation System (GBAS) monitors the signals of Global Navigation Satellite Systems (GNSS) and broadcasts differential correction signals. The GBAS follows Global Positioning System (GPS), the United States-owned GNSS service. An airport installation of GBAS provides navigation and precision approach within a radius of about 23 nautical miles. The current GBAS used in the National Airspace System supports Category I approaches with an accuracy of under one meter in both horizontal and vertical [1].

The FAA-approved GBAS in use, the Honeywell International Satellite Landing System 4000 series (SLS-4000), uses four reference stations, each equipped with an ARL-1900 Multipath Limiting Antenna (MLA) [2]. The antenna performs multipath-limited GPS reception from zenith to 6° above horizon [3,4]; its precursor, ARL-2100, performed reception from zenith to 3° above horizon [5]. According to the FAA [1], approved GBAS only monitor and augment civilian coarse/acquisition (C/A) broadcasts on band L1, broadcast at 1575.42 MHz.

The ARL-1900 and ARL-2100 feature a 19- and 21-element array, respectively [3-6]. The antenna elements are quadrature slanted dipoles with tuning elements to support L1, L2, and L5 bands. The ARL-1900 height is approximately 182.9 cm. Through our investigations, we discovered an approach to design a substitute antenna with less height and fewer elements that still meets the minimum performance requirements for the GBAS.

We propose a substitute antenna, the "Quadrature Self-Cardioid Array" (QSCA). The novel self-cardioid element contributes to multipath mitigation but is small enough for a vertical array. We also developed an array synthesis method that accommodates the element pattern and balances performance among varied requirements. The QSCA accomplishes GBAS needs with 11 array elements and is 97.05 cm tall (approximately 44% shorter than the ARL-1900). The height reduction allows for better wind resistance, and the element quantity reduction permits a simpler array feed system.

II. SUBSTITUTE ANTENNA REQUIREMENTS

Requirements for the substitute MLA are based on current MLA performance descriptions [3-5].

1. $D/U \geq 30$ dB for $0° \leq \theta \leq 84°$.
2. Hemispherical coverage.
3. Point phase center.
4. Point group delay center.
5. Right-hand circular polarization (RHCP) between zenith and horizon ($0° \leq \theta \leq 90°$).

The *D/U*, or desired-to-undesired gain ratio, is defined as the ratio of the gain in positive elevation angles to that of its mirrored negative elevation angle [7], such that $D/U = G(\theta)/G(-\theta)$. The 30 dB requirement for *D/U* is challenging and forces the MLA to include an array in the zenith direction.

Table 1 lists gain requirements for hemispherical coverage [8]. The requirements are set in document DO-301 by the Radio Technical Commission for Aeronautics (RTCA). DO-301 specifically covers airborne antennas [8], but the requirements also work for ground systems.

Submitted On: April 22, 2020
Accepted On: August 8, 2020

https://doi.org/10.47037/2020.ACES.J.351017

Table 1: Gain requirements for a GPS L1 antenna

θ (°)	Minimum Gain (dBic)	Maximum Gain (dBic)
< 75	−2	
80	−3	
85	−5.5	5
90	−7.5	−2
> 120		−10

The point phase center ideally means zero phase center variation (PCV). PCV was defined [7] as:

$$t_{phase}(\omega,\theta,\phi) = c\frac{\varphi(\omega,\theta,\phi)}{\omega}m, \quad (1)$$

where $t_{phase}(\omega,\theta,\phi)$ is the phase delay scaled in meters as a function of the radian frequency, ω, elevation angle, θ, and azimuth angle, ϕ. $\varphi(\omega,\theta,\phi)$ is the phase of the array's electric field, and c is the speed of light. Unfortunately, PCV is never zero in wide-lobe designs such as the GBAS MLA. The point phase center requirement is achieved by using a look-up table in the receiver to compensate for phase changes associated with θ and ϕ angles. The antenna element and array design must avoid sharp phase changes. The phase center for the MLA is in the center array element.

The point group delay center ideally means constant group delay (GD), defined [7] as:

$$t_{group}(\omega,\theta,\phi) = c\frac{d\varphi(\omega,\theta,\phi)}{d\omega}m. \quad (2)$$

Practical antennas allow some group delay change over frequency, but the MLA group delay should change as little as possible throughout the 20 MHz L1 bandwidth. A performance report [4] lists the ARL-1900 RMS carrier-delay variation as ≤ 0.007 m and code-delay variation as ≤ 0.025 m. The estimates are based on measurements of four MLAs over 24 hours and thus are dependent on receiver performance. Any MLA substitute should contain an antenna and associated RF networks with at least a 20 MHz bandwidth to minimize error.

To maintain RHCP coverage, the RH/LH polarization ratio must be positive for 0° ≤ θ ≤ 90°. RH/LH are respective magnitudes of RHCP and LHCP radiation. However, a positive ratio alone may not be adequate [9]. As discussed by Lopez [9], non-ground reflections such as lateral reflections can be larger than direct signals, with the potential to cause severe errors. Therefore, the RH/LH ratio should be as large as possible, particularly for angles near the horizon.

III. ARRAY DESIGN FOR MINIMUM PHASE CHANGE

A linear array in the zenith direction is needed to meet the 30 dB *D/U* requirement. This array will have no impact on the RHCP requirement, leaving that need to the antenna element. To meet other requirements, the array must have hemispheric coverage and minimal phase change over its coverage.

Array Factor (*AF*) can be treated separately from the antenna gain pattern if every element in the array experiences the same near field, which requires element distance to be constant [5]:

$$\begin{aligned} &E(\theta,\phi) = g(\theta,\phi)AF(\theta),\\ &E(\theta,\phi) = Radiation\ Pattern,\\ &g(\theta,\phi) = Element\ Factor\ Pattern. \end{aligned} \quad (3)$$

$E(\theta,\phi)$ is the radiation pattern of the entire antenna, inclusive of element/array effects; $g(\theta,\phi)$ is the radiation pattern of one antenna element, treated as though placed at the point phase center and excited with 0 dB.

Suppose we have a linear array with *M* number of elements, each with distance d_m spacing from center, and amplitude and phase defined by $\overrightarrow{a_m}$. $k = 2\pi/\lambda$. The *AF* for such a configuration is:

$$AF(\theta) = \sum_{m=0}^{M} \overrightarrow{a_m} e^{jkd_m cos\theta}. \quad (4)$$

The complex exponential terms have phases that change according to θ. This can result in large PCV, especially when d_m becomes large. To eliminate the phase changes, the following trigonometric identities are used:

$$\begin{aligned} e^{jkd_m cos\theta} + e^{-jkd_m cos\theta} &= 2cos(kd_m cos\theta),\\ e^{jkd_m cos\theta} - e^{-jkd_m cos\theta} &= 2jsin(kd_m cos\theta). \end{aligned} \quad (5)$$

To use the identities, the array elements are split into pairs; each pair has one element above array center and the other below at an equal distance. Each element has a unique number *n*, with $n = 0$ as the center element, $n > 0$ above center, and $n < 0$ below center. Paired elements have a pair number *p* and distance d_p from the array center, *p* equaling the number of pairs. Each pair has a common amplitude, but their feed phases are conjugates, as given by W_p. One center element is added to help shape the array factor, making this an odd-number array:

$$\begin{aligned} &d_0 = 0, \quad d_n = -d_{-n} = d_p,\\ &\overrightarrow{a_n} = \overrightarrow{W_p}, \quad \overrightarrow{a_{-n}} = \overrightarrow{W_p^*},\\ &\overrightarrow{W_0} = X_0, \quad \overrightarrow{W_p} = X_p + jY_p,\\ &R(p,\theta) = kd_p cos\theta, \end{aligned} \quad (6)$$

$$AF(\theta) = X_0 + \sum_{p=1}^{P} \left[2Y_p sinR(p,\theta) + 2X_p cosR(p,\theta)\right].$$

The MLA array *AF* (θ) contributes to no phase changes over θ because its weights are limited to conjugate pairs.

IV. SINE PAIR ARRAY DESIGN FOR HIGH *D/U* AND STEADY GAIN

If an *AF* pattern was a unit step function, with value of 1 when $\theta \le 84°$ and 0 when $\theta \ge 96°$, *D/U* would be infinity throughout the covered area. The array weights needed would resemble the well-known Fourier series:

$$\begin{aligned} &d_p \approx (2p-1)0.4532\lambda,\\ &X_0 = 1,\ Y_0 = 0, X_{p>0} = 0,\\ &Y_p = F(p)[Approximating\ Function]. \end{aligned} \quad (7)$$

Such an array can be called a "Sine Pair Array" (SPA). Active element spacing is 0.4532λ for the center three elements and 0.9064λ beyond that. Each element must experience the same near field, so passive elements are inserted as needed to maintain an overall 0.4532λ. Two passive elements are placed at the ends of the array to assure near field uniformity, akin to a recommended design [3]. 0.4532λ is chosen over λ/2 to avoid a performance gap around zenith and nadir.

An iterative solver was designed to synthesize SPA weights to approximate the unit step function. The solver achieved gain within requirements ($D/U > 30dB$ when $\theta \leq 84°$), with 9 active and 10 passive elements. The weights are $\overrightarrow{W_0} = 1, \overrightarrow{W_1} = 0.6290, \overrightarrow{W_2} = 0.1887, \overrightarrow{W_3} = 0.0917, \overrightarrow{W_4} = 0.0592$. Estimating element length as equal to d_L and using the GPS L1 λ of 19.03 cm, the total length is 172.5 cm, close to the BAE ARL-1900 height of about 6 feet (182.9 cm) [2]. The *AF* pattern seen in Fig. 1 closely matches the 11-active-element ARL-2100 *AF* [5], although the latter has a cutoff closer to the horizon.

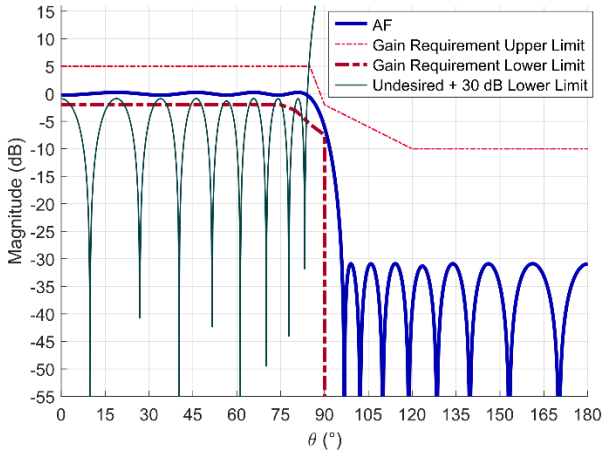

Fig. 1. Performance of SPA with nine active isotropic elements with element spacing of 0.4532λ.

The 30 dB *D/U* requirement was graphed by mirroring the *AF* at negative angles and adding 30 dB, representing the lower limit for gain at which the corresponding *AF* is compliant. Gain is well within the required passing zone, while *D/U* is much closer to its boundaries and ultimately fails when $\theta > 84°$.

V. *D/U* IMPROVEMENT VIA ANTENNA ELEMENT

The authors hypothesized that the number of active array elements could be reduced if the antenna element contributed to *D/U*. The Element Factor Pattern over θ for the ARL-2100 is nearly isotropic. Figure 2 shows an approximation of the pattern and its corresponding *D/U*. Detailed information is available in the literature [6]. RHCP coverage is maintained in the upper atmosphere; however, the ARL-2100 element does not provide any substantial *D/U* benefit or deficit.

Also included in Fig. 2 is the element gain and *D/U* of a λ/2 long vertical dipole, like other proposals [10] and uses [11,12]. The dipole doesn't contribute to *D/U*, but its nulls at zenith and nadir allow it to integrate easily with another antenna to cover zenith.

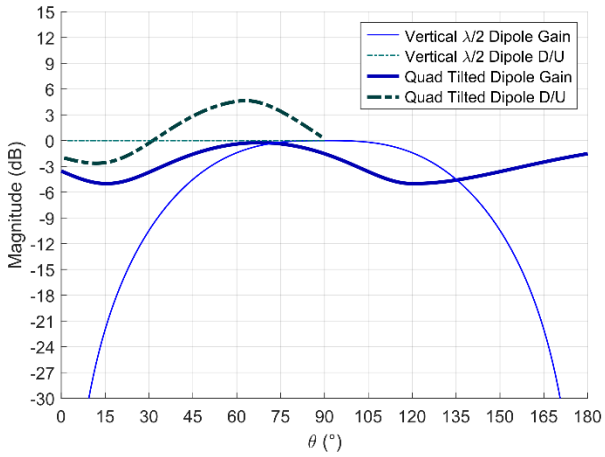

Fig. 2. Approximation of gain and *D/U* of a vertical λ/2 dipole and a quadrature tilted dipole element.

A. Previous MLA antenna element *D/U*

Thornberg et al. [11,12] designed a 14-element (vertical) dipole array MLA, which was measured to cover $55° \leq \theta \leq 90°$. The height was not reported, but a 16-element version was described as being 256.54 cm (101 in.) tall. A helibowl high zenith antenna (HZA) was added to cover $0° \leq \theta \leq 55°$. The HZA achieves a minimum −32 dB *D/U* at 55°. It is composed of crossed V-dipoles, a reflecting counterpoise, a shaped reflector, a quarter-wave RF choke, and a precisely designed "shaped absorber." The HZA achieves *D/U* without arraying. Unfortunately, it is 58.42 cm (23 in.) tall and thus unsuitable for a vertical array.

In another proposed MLA design [13], a three-element multipath rejecting array was measured that featured separate, interleaved elements for L1 and L2. Each element is a turnstile with four horizontal arms. The element pattern has not been listed, but the design's up-to-down gain ratio performance is attributed to its array weights. This design is 32.4 cm (12.75 in) and achieves a far more relaxed *D/U* requirement.

Rolled edge ground planes have had some success, but their large diameters > 4λ attenuate the signal to lower array elements and thus violate the identical near-field requirement. Choke rings are slightly better with diameters around 2λ, but heights around λ/4 leave little space for the actual element before reaching the λ/2 element spacing. Both rolled edge ground planes and

choke rings are heavy and would require adaptation to work with a vertical array.

B. *D/U* benefit of a cardioid array

One method of achieving *D/U* is placing a null at nadir with a cardioid array. Two identical elements are oriented in a straight line with λ/4 distance between them. Their signals are added with equal amplitude and a 90° phase difference. The cardioid array eliminates the signal in the backward direction for the design frequency. The cancellation technique is not exclusive to the classic λ/4 cardioid pair; any distance d_c between paired elements can be used if proper phase difference p_c is applied. The required formula is:

$$p_c = 180° - \frac{360° \cdot d_c}{\lambda}, \qquad (8)$$

$$G_c = 1 + cos\left(p_c - \frac{cos\theta \cdot 360° \cdot d_c}{\lambda}\right).$$

Table 2 shows several examples of pair distances d_c and their voltage gains G_c at example angles. Gain is best at λ/4 spacing, which is the classic cardioid pattern, but any spacing between λ/8 and 3λ/8 still has useable gain. *D/U* is zero at λ/2 spacing, which is the classic omnidirectional pattern. For all distances, *D/U* is outstanding at very low θ and theoretically infinity at zenith. *D/U* is poor at other angles. *D/U* increases rapidly as distance decreases and is usable at 4λ/9 or less.

The cardioid array has useful *D/U* over a small angle. The cardioid array can be made with short vertical spacing that is conducive to further arraying to add more *D/U*. A similar concept of array hybridization has been described [14]. Unfortunately, this approach results in a pattern, an array of arrays, that would require many active elements.

Table 2: Voltage gain of isotropic pair phased for cardioid behavior

Space (λ Length)	Phase Delta (°)	Observation Angle (°)				
		0	20	90	160	180
		Voltage Gain (dB)				
1/18	160	−12.6	−13.1	−24.4	−73.1	−∞
1/8	135	0	−0.42	−10.7	−59.0	−∞
1/4	90	6.02	6.00	0	−47.0	−∞
3/8	45	0	1.15	4.65	−39.9	−∞
4/9	20	−12.6	−9.06	5.75	−37	−∞
1/2	0	−∞	−34.9	6.02	−34.9	−∞

VI. SELF-CARDIOID ANTENNA

We designed a "Self-Cardioid Antenna" (SCA) that achieves cardioid-like behavior without explicitly arraying two elements. A meandering element is mounted and fed at the edge of a ground block. The element's other end is terminated with a similar ground block. Each ground block and horizontal section of the meander line receive horizontally polarized energy. Each reception point experiences different delays and reflections before the transmission of horizontal energy into the feed point. With modern antenna design programs and parametric sweeps, proper dimensions can achieve a balanced design that cancels out most LHCP energy from the nadir direction. This balanced design is the SCA.

A. Quadrature design

Arranging four SCA in a square pattern with progressive 90° feeds yields one QSCA element. The feed network produces RHCP in the upper hemisphere while eliminating LHCP at zenith and RHCP at nadir. As each SCA element cancels LHCP at nadir, the QSCA element has a complete null at nadir. The cubic design fits outside of a square mast supporting vertical array.

Figure 3 shows a QSCA design for L1. The element height (and distance between elements) is 0.425λ. (See Table 3 for dimensions in cm.) Each SCA is fed at its top, grounded to the mast at its bottom, and composed of nine sequential conductive segments. The feed points are located at mast entry points so that impedance-matching and feed networks fit inside the mast along with the RF cabling. This design is a complex geometry with precision lengths. The use of a cubic arrangement places the intricate segments in four planes. Each plane can be realized with good precision with printed circuit board fabrication, like a cubic antenna design proposed by Merulla [15].

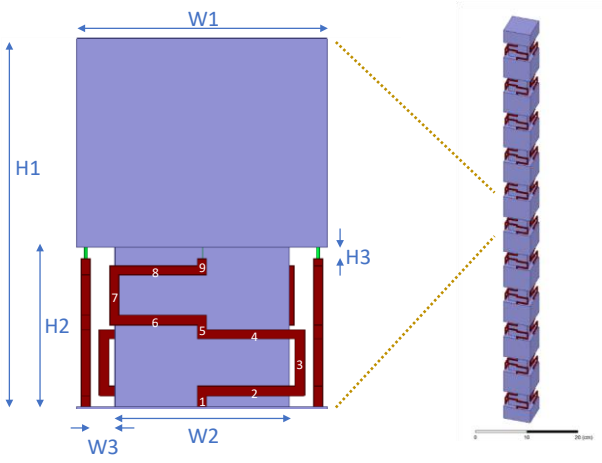

Fig. 3. Left side shows a QSCA element with dimensions and right side shows an 11-element array.

B. Electromagnetic simulation

Testing our design required several simulations with parametric sweeps of the section lengths to find dimensions to achieve resonance and self-cardioid behavior at L1. We used Ansys Electromagnetics Suite 19.2, Electronics Desktop 2018.2.0, HFSS for antenna

simulations. The full array was electromagnetically modeled, with only the center element excited. Foster and Wicks [16] demonstrated that full array models in HFSS showed slight performance differences in contrast to the less computationally intense geometric boundary symmetry options. Tokan and Gunes [17] described the importance of modeling the mutual coupling that occurs between non-isotropic array elements.

Table 3: Dimensions in cm of QSCA element

H1	8.08775	H2	3.5	H3	0.25
W1	5.5	W2	3.81	W3	0.545
Segment Cross-section 0.2 x 0.2					
Segment Lengths					
#1	0.345	#2	2.15	#3	1.25
#4	2.15	#5	0.305	#6	1.92425
#7	1.1	#8	1.92425	#9	0.25

Simulation results show the sub-element impedance is 3.7024 **Ω** + *j*0.0630 **Ω**. Figure 4 shows the simulation results for element factor pattern, polarization, and *D/U* of one QSCA element.

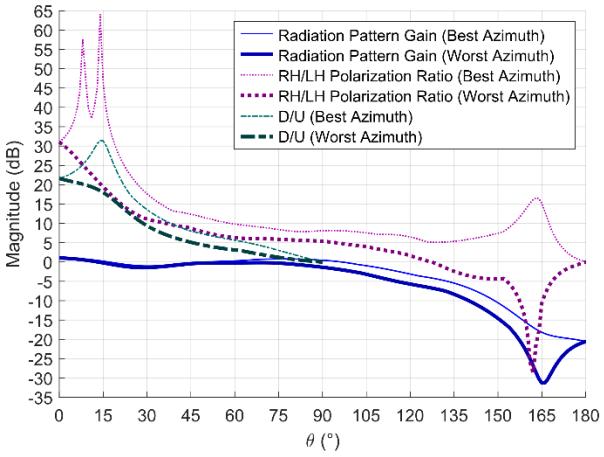

Fig. 4. Gain, polarization, and *D/U* of QSCA element.

All three parameters have good values throughout the upper hemisphere. *D/U* is particularly good near the zenith. Performance changes little across all phi angles, a benefit of having elements that do not radiate far from the vertical axis. The maximums and minimums of *D/U* do not align perfectly with the radiation pattern; they must be calculated from the element factor pattern for all phi.

VII. ARRAY IMPROVEMENTS THAT COMPLEMENT QSCA

We made several improvements to complement the QSCA and reduce the number of array elements. First, we included the QSCA element factor pattern in the array synthesis and set the iterative solver to evaluate the overall radiation pattern. The factor pattern was taken from a simulation of a single active element flanked by passive elements like it is in an array. Second, we modified the iterative solver from mere gain pattern matching. Both the SPA and ARL-2100 use array synthesis to shape the *AF* pattern to an approximation of unit step gain. This pattern keeps *AF* well within the gain requirement pass zone throughout all angles, only coming close to the limits at θ = 90°. Meanwhile, *D/U* is closer to its limit. Thus, *AF* over-complies with the gain requirements but is barely compliant with the *D/U* requirement. The new iterative solver evaluated prospective array weights to determine when a resulting radiation pattern had *D/U* > 30 dB when $\theta \leq 84°$. We then re-evaluated the pattern to see how closely it resembled the unit-step function for $\theta \leq 84°$. We call this process, "Mixed Goal Array Synthesis."

The third improvement was varying the feed weight phases to add cosine-based functions $2X_p cosR(p,\theta)$. These were not included in the SPA, as they are not part of the Fourier transform of a unit step. The functions can increase *D/U* near the horizon, but at the cost of decreasing the gain, increasing or decreasing gain in other areas, and decreasing *D/U* in other areas, including near the zenith. The other improvements balance out these costs. The new feed phases are still complex conjugates. The fourth improvement was to make $d < d_L$. The third improvement introduced cosine terms that eliminated previous SPA symmetry and also decreased *D/U* near zenith, which can be partially mitigated by reducing *d*. No exact formula exists for ideal *d* when adding cosine terms, but experimental values between 0.45λ and 0.3λ yielded good results. QSCA uses 0.425λ.

VIII. QSCA WEIGHTS AND PERFORMANCE

From each simulation, the most important data was the worst *D/U* among all ϕ, for each θ. This data requires comparisons of gain data among different angles, with sorting and searching, actions not supported in the user interface of most electromagnetic software simulators. Thus, the gain data for each steradian was exported after each simulation into Excel. Excel formulas then computed the worst *D/U* data, which was exported to MATLAB for further processing. A local ground reflectivity and polarization loss factor of 3 dB was applied to *D/U* [5]. The 1° steradian resolution results in 129,600 gain data values per simulation, plus the refined worst *D/U* data. Excel's error checking and conditional formatting are invaluable tools for finding errors that are imperceptible in simple gain graphs.

The MATLAB iterative solver used the worst *D/U* data, as well as the original gain data, to find array weights specific to the SCA design. Only three weights

were needed, equating to five active elements. Six passive elements were added, for a total of 11 elements. Figures 5 and 6 show QSCA radiation and *D/U* patterns versus requirements. Both figures show compliance to requirements except for angles beyond the 84° θ cutoff. Both patterns come close to requirement limits, showing our minimization techniques achieved a proper balance of performance. The total length of the QSCA is 97.05 cm, approximately 44% shorter than the ARL-1900. The QSCA requires 5 active (11 total) elements, versus 9 active (19 total) elements in the ARL-1900.

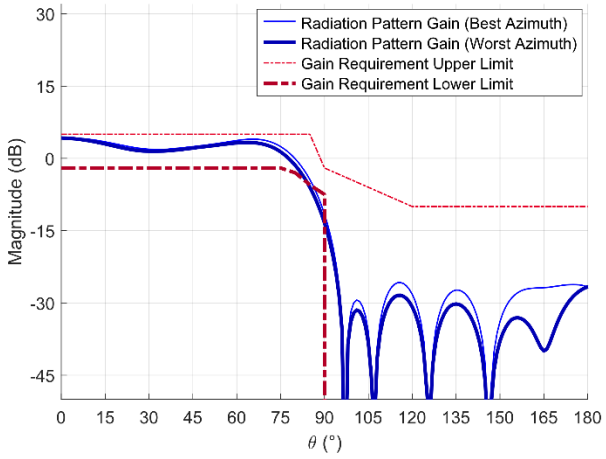

Fig. 5. QSCA radiation pattern and requirements.

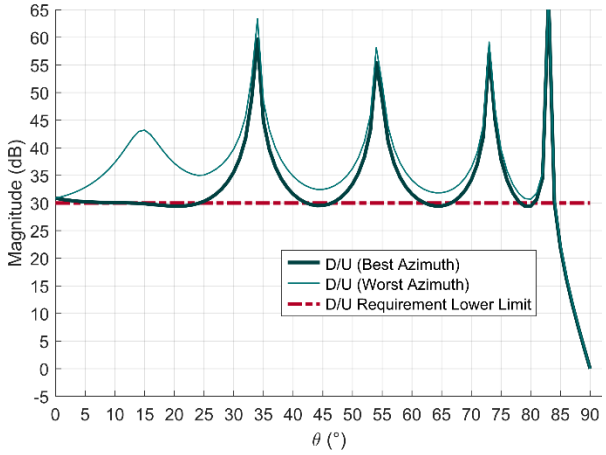

Fig. 6. QSCA *D/U* pattern and requirements.

The QSCA weights are $X_0 = 1, X_1 = -0.1875$, $Y_1 = 0.5773, X_2 = -0.1354, Y_2 = 0.07444$. X_1 and Y_1 can be combined via a trigonometric identity to yield one amplitude and one phase. X_2 and Y_2 can be combined likewise. This trigonometric identity is:

$$A\cos\theta + B\sin\theta = \sqrt{A^2 + B^2}\,\sin\left(\theta + \tan^{-1}\frac{A}{B}\right). \quad (9)$$

Table 4 contains a simplified list of the amplitudes, feed phases, and distances from the center for all the QSCA elements.

Table 4: QSCA amplitudes, phase excitations, and distances

Element No.	Excitation		Distance
	Amplitude (Voltage)	Phase (Degrees)	From Center (cm)
1 (bottom)	0		−40.43875
2	0		−32.351
3	0.15453	−151.199	−24.26325
4	0		−16.1755
5	0.607192	107.9932	−8.08775
6	1	0	0
7	0.607192	−107.9932	8.08775
8	0		16.1755
9	0.154353	151.199	24.26325
10	0		32.351
11 (top)	0		40.43875

IX. EXPERIMENTAL VERIFICATION

We built a prototype of one QSCA element to measure its performance. A single element prototype was chosen for the ease of construction and adjustment and to focus on proving the novel self-cardioid behavior. A mast was constructed from aluminum, with printed circuit boards forming the mast sides and the sub-elements. Double-sided FR4 (1 oz., 0.15748 cm [0.062 in] thick) was chosen for its strength and quick turnaround time. The circuit board has many cut edges. We applied MG Chemicals silver-coated copper conductive coating, #843WB, on the edges.

We employed Feko 2019 for the electromagnetic simulations of the prototype. This variation in electromagnetic simulation software helped demonstrate that the self-cardioid behavior was not a byproduct of modeling approximations. PCB123 software was used for the circuit board design. A quadrature feed board, consisting of two hybrid branch-line couplers and one hybrid ring coupler, fed the four elements with progressive 90° phases. This feed board was also constructed out of FR4. An "L" network, consisting of 1.3 nH series and 1.5 pF shunt, was installed for each sub-element. A PS100 RF Vector Antenna Analyzer Meter revealed each sub-element matched to 50 Ω with better than 13 dB return loss.

The prototype was installed and tested at the Oakland University (Rochester, Michigan) Automotive Antenna Measurement Instrumentation (AAMI), which measures one hemisphere at a time. Measurements were made for both RHCP and LHCP. The antenna was

installed in normal orientation and upside-down. All measurements were repeated with the antenna raised an additional 5.08 cm (2 in.) to reveal multipath capability.

Data was linear-averaged across all the phi points and again for the different heights. Figure 7 shows the results. The gain was disappointing at medium to low elevation, and multipath in the measurement system was eliminated. *D/U* was 15.96 dB at the zenith and remained positive through 55° θ, demonstrating self-cardioid behavior.

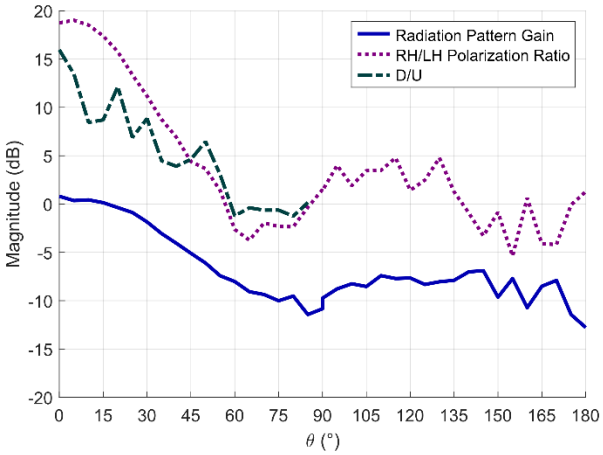

Fig. 7. QSCA single element prototype performance measurements, showing self-cardioid behavior.

Fig. 8. QSCA single element prototype with quadrature feed board, tested at AAMI.

Figure 8 shows the prototype at AAMI, mounted on top of a measurement stand situated in the middle of a turntable. The quadrature feed board is mounted below and to the side. The reference antenna is mounted on the gantry arm that is visible in the background.

X. CONCLUSIONS

Applications such as GBAS require the use of MLAs to achieve near-hemispheric coverage of high *D/U* ratio and moderate gain. Previous MLA array synthesis methods attempted to match the gain pattern to an ideal, which resulted in over-performance of gain and moderate performance of *D/U* per quantity of array elements. Our mixed-goal array synthesis gives a better balance of gain and *D/U* performance. Adding cosine functions, reducing element distances, and developing the self-cardioid antenna element provided *D/U* improvements. The QSCA antenna achieved gain and the required *D/U* performance while achieving a 44% reduction in the number of array elements and the overall size.

REFERENCES

[1] Federal Aviation Administration, "Satellite navigation − Ground Based Augmentation System (GBAS)," https://www.faa.gov/about/office_org/headquarters_offices/ato/service_units/techops/navservices/gnss/laas/, April 2018, accessed Feb. 2020.

[2] Federal Aviation Administration, "Ground Based Augmentation System: Performance Analysis and Activities Report, July 1 – October 31, 2017," Author, Washington, DC, 2017.

[3] A. R. Lopez, "LAAS/GBAS ground reference antenna with enhanced mitigation of ground multipath," *Proceedings of the 2008 National Technical Meeting of the Institute of Navigation*, San Diego, CA, pp. 389-393, Jan. 2008.

[4] A. R. Lopez, "GPS landing system reference antenna," *IEEE Antennas and Propagation*, vol. 52, no. 1, pp. 104-113, Feb. 2010.

[5] A. R. Lopez, "GPS ground station antenna for local area augmentation system, LAAS," *Institute of Navigation National Technical Meeting*, Anaheim, CA, pp. 738-742, Jan. 2000.

[6] A. R. Lopez, "Differential GPS ground reference antenna for aircraft precision approach operations – WIPL design," *17th Annual Review of Progress in Computational Electromagnetics*, Naval Post-graduate School, Monterey, CA, Mar. 2001.

[7] M. S. Sharawi and D. N. Aloi, "Null steering approach with minimized PCV and GD for large aperture vertical antenna arrays," *IEEE Trans-actions on Antennas and Propagation*, vol. 55, no. 7, pp. 2120-2123, July 2007.

[8] B. R. Rao, "Introduction to GNSS antenna performance parameters," in B. R. Rao, W. Kunysz, R. Fante, and K. McDonald, editors, *GPS/GNSS Antennas*, Artech House, Norwood, pp. 1-62, 2013.

[9] A. R. Lopez, "LAAS reference antennas – Circular polarization mitigates multipath effects," *Institute*

of Navigation 59th Annual Meeting / CIGTF 22nd Guidance Test Symposium, Albuquerque, NM, pp. 500-506, 2003.

[10] M. Braasch, "Optimum antenna design for DGPS ground reference stations," *Proceedings of the 7th International Technical Meeting of the Satellite Division of The Institute of Navigation (ION GPS 1994)*, Salt Lake City, UT, pp. 1291-1297, 1994.

[11] D. B. Thornberg, D. S. Thornberg, M. F. DiBenedetto, M. S. Braasch, F. van Graas, and C. Bartone, "The LAAS integrated multipath limiting antenna (IMLA)," *Proceedings of the 15th International Technical Meeting of the Satellite Division of The Institute of Navigation (ION GPS 2002)*, Portland, OR, pp. 2082-2092, 2002.

[12] D. B. Thornberg, D. S. Thornberg, M. F. DiBenedetto, M. S. Braasch, F. van Graas, and C. Bartone, "LAAS integrated multipath limiting antenna," *NAVIGATION*, vol. 50, no. 2, pp. 117-130, 2003.

[13] C. Counselman, "Multipath-rejecting GPS antennas," *Proceedings of the IEEE*, vol. 87, no. 1, pp. 86-91, Feb. 1999.

[14] O. Gassab and A. Azrar, "Novel mathematical formulation of the antenna array factor for side lobe level reduction," *ACES Journal*, vol. 31, no. 12, pp. 1452-1462, Dec. 2016.

[15] E. J. Merulla, "Low-profile dual-band emulated GPS constellation antenna," *2017 International Applied Computational Electromagnetics Society Symposium*, Italy, 2017.

[16] P. R. Foster and A. E. Wicks, "Modeling the RF performance of a small array," *Applied Computational Electromagnetics Society Journal*, vol. 21, no. 3, pp. 291-298, Nov. 2006.

[17] F. Tokan and F. Gunes, "Mutual coupling compensation in non-uniform antenna arrays using inter-element spacing restrictions, *ACES Journal*, vol. 26, no. 7, pp. 596-602, July 2011.

James A. Quinlan received a Bachelor of Science degree in Electrical Engineering (2002) and Masters' degrees in Electrical and Computer Engineering (2005) from Oakland University, Rochester, Michigan, USA. He is employed by General Dynamics Land Systems, where his work involves vehicle system integration, GPS performance, radiation, and survivability. He has several years of experience in managing computer engineering laboratories. Quinlan is a member of the Applied Computational Electromagnetics Society, Institute of Navigation, and Institute of Electrical and Electronics Engineers (IEEE).

Daniel N. Aloi received his B.S. (1992), M.S. (1996), and Ph.D. (1999) degrees in Electrical Engineering from Ohio University, located in Athens, Ohio, USA. He is a Professor in the Electrical and Computer Engineering Department at Oakland University (OU) and Founder and Director of OU's Applied Electromagnetics and Wireless Lab (AEWL). Aloi's research interests reside in applied electromagnetics with an emphasis on antenna measurements, modeling/analysis, and design. He is a member of the Applied Computational Electromagnetics Society (ACES) and the Institute of Navigation (ION) and a senior member of the Institute of Electrical and Electronics Engineers (IEEE). Aloi has authored or coauthored over 100 technical papers and is the primary inventor or coinventor on several patents.